

Behavior of UHPC-RW-RC wall panel under various temperature and humidity conditions

Xiangguo Wu^{*1,2}, Shiyuan Yu², Xiaokun Tao³, Baochun Chen¹, Hui Liu⁴,
Ming Yang³ and Thomas H.-K. Kang^{**5}

¹College of Civil Engineering, Fuzhou University, Fuzhou, 350108, China

²Key Lab of Structures Dynamic Behavior and Control of the Ministry of Education, Key Lab of Smart Prevention and Mitigation of Civil Engineering Disasters of the Ministry of the Industry and Information Technology, Harbin Institute of Technology, Harbin, 150090, China

³Hebei Construction Material Vocational & Technical College, Qinhuangdao, Heibei, 066004, China

⁴Qinhuangdao Municipal Building Material Group Co., Ltd., Qinhuangdao, Heibei, 066000, China

⁵Department of Architecture & Architectural Engineering and Engineering Research Institute, Seoul National University, Seoul, 08826, Republic of Korea

(Received January 19, 2020, Revised April 14, 2020, Accepted April 3, 2020)

Abstract. Mechanical and thermal properties of composite sandwich wall panels are affected by changes in their external environment. Humidity and temperature changes induce stress on wall panels and their core connectors. Under the action of ambient temperature, temperature on the outer layer of the wall panel changes greatly, while that on the inner layer only changes slightly. As a result, stress concentration exists at the intersection of the connector and the wall blade. In this paper, temperature field and stress field distribution of UHPC-RW-RC (Ultra-High Performance Concrete - Rock Wool - Reinforced Concrete) wall panel under high temperature-sprinkling and heating-freezing conditions were investigated by using the general finite element software ABAQUS. Additionally, design of the connection between the wall panel and the main structure is proposed. Findings may serve as a scientific reference for design of high performance composite sandwich wall panels.

Keywords: finite element analysis; modeling; simulation; ultra-high performance concrete; rock wool; sandwich wall panel; temperature; humidity

1. Introduction

With the advent of prefabricated buildings, utilization and application of pre-fabricated exterior wall panels for projects of convenience also arose. Composite sandwich hanging panels are the main type of non-bearing components in these assembly structures. Because the external wall panel is affected by the environment, it is very important to study weatherproof performance of the prefabricated external wall panel in evaluating its design performance, especially temperature change and its effect under external thermal-humidity and thermal-cold action (i.e., high temperature and low temperature cyclic action). A significant amount of research has been done on thermal insulation and the energy-saving effect of external wall panels worldwide, but research on their structural behavior, especially on temperature stress, is necessary. Note that the design and service life of concrete components and joint connectors in the hanging wall panel system should be the same as that of the main structure (JGJ/T 45-2018). In China's "external wall insulation engineering technical specifications", the design life of the external thermal

insulation system of the external wall is less than 25 years under the conditions of proper use and normal maintenance.

However, limited research is available on relevant topics except a few (Lie *et al.* 1996, Shin *et al.* 2002, Zhang *et al.* 2014, Zheng *et al.* 2014, Shaikh and Taweel 2015, Ximenes *et al.* 2015, Uygunoğlu *et al.* 2016, Zhang *et al.* 2016, Vilhena *et al.* 2017, Sulakatko and Vogdt 2018, Zhang *et al.* 2019, Bonner *et al.* 2020). Therefore, in this paper, the ABAQUS finite element software was used to create a three-dimensional transient thermal structure coupling model of high performance multi-functional composite sandwich wall panels. To which, the temperature field and stress distribution of the wall panels in the process of high temperature-water spraying and heating-freezing were investigated. Time dependent temperature field and stress field of the wall panels under the action of cold-heat and freeze-thaw were calculated. This study provides a scientific reference for analysis and design of weatherproof performance of composite sandwich exterior wall panels.

2. Composition and theoretical basis of wall panel

2.1 Wall panel composition

Ultra-high performance concrete (UHPC) is an advanced cement-based composite material with high durability, mechanical properties and workability due to use

*Corresponding author, Professor

E-mail: wuxiangguo@hit.edu.cn

**Co-corresponding author, Professor

E-mail: tkang@snu.ac.kr

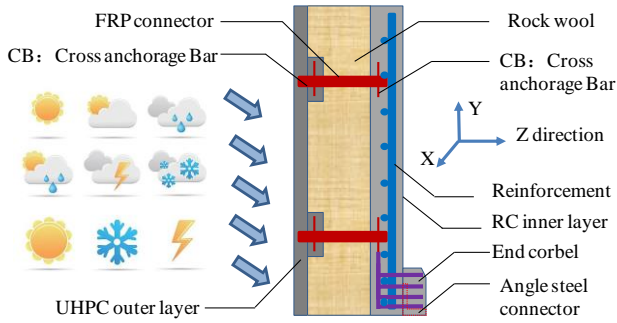


Fig. 1 Composition and construction of composite wall panel

of superplasticizer, active mineral admixture and fiber reinforced toughening multiple technologies. Its design compressive strength can reach 100-200 MPa. The UHPC-RW-RC composite wall panel is formed by using UHPC as the outer layer of the external wall hanging panel, high density rock wool (RW) as the insulation core material and reinforced concrete as the inner wall layer. The UHPC exterior wall characteristics include: lightweight; crack resistance; and durability for long-life. Basic concepts of UHPC-RW-RC composite sandwich exterior wall panel and corresponding connection and construction forms are shown in Fig. 1.

2.2 Theoretical and methodological basis

The internal temperature of composite wallboard varies

little in the directions of length X and width Y . Ignoring the difference of heat transfer between these two directions, the heat conduction equation of wallboard can be simplified to a one-dimensional heat conduction equation in the Z direction, wall thickness, i.e.

$$\frac{\partial T(x,t)}{\partial t} = \frac{\lambda}{\rho c} \frac{\partial^2 T(x,t)}{\partial t^2} \tag{1}$$

Where: $T(x, t)$ is the temperature at x position and t .

Given the boundary conditions and time, the temperature field in the Z direction of the wall thickness can be obtained by solving Eq. (1) and temperature at each position inside the wall can be obtained. Temperature stress analysis is carried out in accordance with elastic theory (Bonner *et al.* 2020). Expression of the temperature stress field is as follows

$$\begin{aligned} \varepsilon_x &= \frac{1}{E}[\sigma_x - \mu(\sigma_x + \sigma_z)] + \alpha\Delta T; \quad \gamma_{xy} = \frac{2(1+\mu)}{E} \tau_{xy} \\ \varepsilon_y &= \frac{1}{E}[\sigma_y - \mu(\sigma_y + \sigma_z)] + \alpha\Delta T; \quad \gamma_{yz} = \frac{2(1+\mu)}{E} \tau_{yz} \\ \varepsilon_z &= \frac{1}{E}[\sigma_z - \mu(\sigma_x + \sigma_y)] + \alpha\Delta T; \quad \gamma_{zx} = \frac{2(1+\mu)}{E} \tau_{zx} \end{aligned} \tag{2}$$

Where: ΔT is the calculated temperature difference, μ is the Lamé's constant, $\sigma_x, \sigma_y,$ and σ_z are the positive stress components, $\tau_{xy}, \tau_{yz},$ and τ_{zx} are the shear stress components, $\varepsilon_x, \varepsilon_y,$ and ε_z are the positive strain components, and $\gamma_x, \gamma_y,$ and γ_z are the shear strain components.

The above formula is a calculation formula of one-

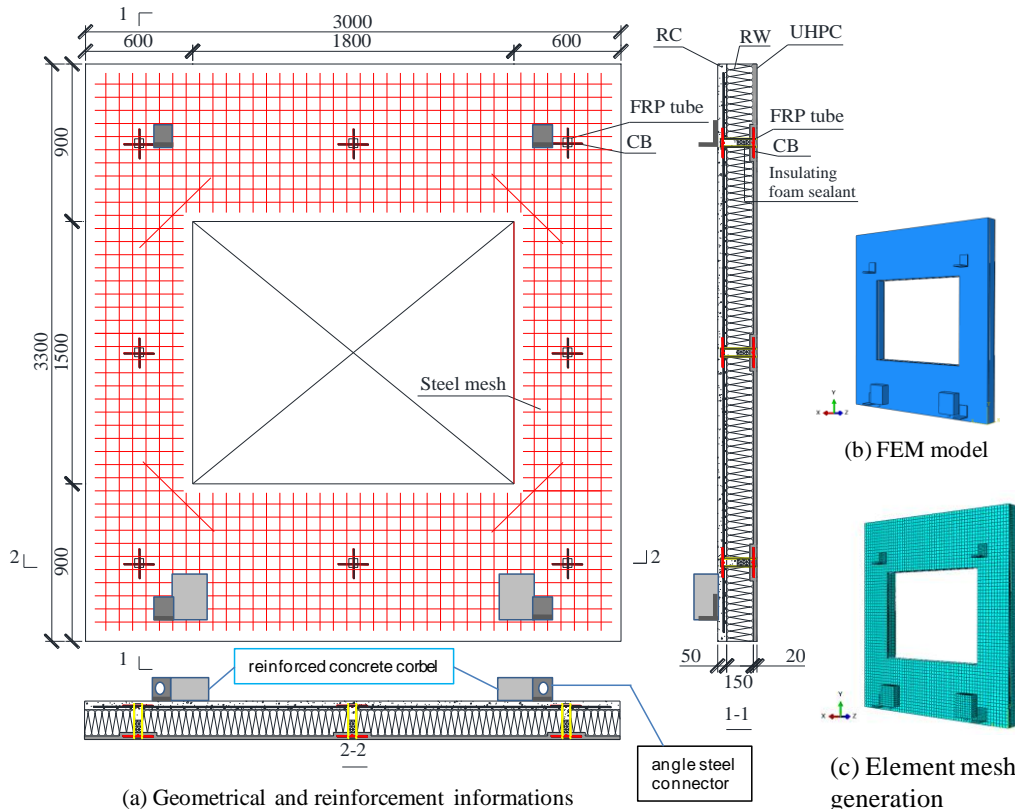


Fig. 2 Basic information of wall panel specimens and FEM model (Unit: mm)

Table 1 Material properties

Material*	Δx	ρ	c	λ	α	E	ν
UHPC	20	2450	920	1.74	11	43	0.18
RW	140	120	1.22	0.04	1	5.2×10^{-3}	0.13
Concrete	50	2500	920	1.74	10	30	0.2
Steel	-	7850	0.48	58.2	10	200	0.31
FRP	-	1820	1.26	0.52	10	28	0.26

Where: Δx is the panel layer thickness (mm), ρ is the density ($\text{kg}\cdot\text{m}^{-3}$), c is the specific heat capacity ($\text{J}\cdot\text{kg}^{-1}\cdot\text{C}^{-1}$), λ is the heat conductivity ($\text{W}\cdot\text{m}^{-1}\cdot\text{C}^{-1}$), α is the coefficient of linear expansion (10^{-6}C^{-1}), E is the elastic modulus (GPa), and ν is the Poisson's ratio.

dimensional temperature conduction and a simplified model. Based on this, the three-dimensional temperature conduction model is used for finite element analysis as in the following.

3. Finite element model

3.1 Geometrical conditions

Geometric dimensions and structural layout of the hanging panel of the UHPC-RW-RC composite sandwich exterior wall are shown in Fig. 2(a). Based on the experimental wall panel, the finite element analysis model was established. In the model, the effect of the end cross anchorage bar (CB) is neglected, and the FRP tube is fixed directly in the inner and outer layers. To simplify the model, RW is assumed fixed directly to the inner and outer layers of wall panels since it has very little stiffness. Four angle steel connectors are installed in the inner layers of the wall panel to act as a horizontal sliding brake. Two reinforced concrete corbels are arranged at the lower part of the inner layer and connected with the support of steel anchor bolts. The finite element model is shown in Fig. 2(b).

3.2 Material properties

It is assumed that all materials of wall panel conform to the assumption of uniform continuity and isotropy, and there is no gap and relative sliding between the material layers. Because the temperature stress of all components except RW is far less than the maximum stress in the elastic stage, the components are modeled by elastic method, and the mechanical and thermal properties of materials(GB 50176-2016) are defined by referring to Table 1.

3.3 Constraint setting and meshing

Constraints are set at the corbel and horizontal angle steel joints of the wall panel. The wall panel adopts a three-dimensional thermo-coupled solid element, which is an 8-node hexahedron element suitable for temperature analysis. The inner and outer wall layers and sandwich layer are divided into four grids along the thickness direction of the wall. The size of grids along the X and Y directions of the wall is 50 mm. The gridding is shown in Fig. 2(c). The

Table 2 Surface environmental temperature of wall panel under two working conditions

High temperature-spray		Heating-freezing conditions	
Time t (h)	Temperature T ($^{\circ}\text{C}$)	Time t (h)	Temperature T ($^{\circ}\text{C}$)
0	18	0	18
1	70	1	50
3	70	8	50
4	15	10	-20
6	18	24	-20

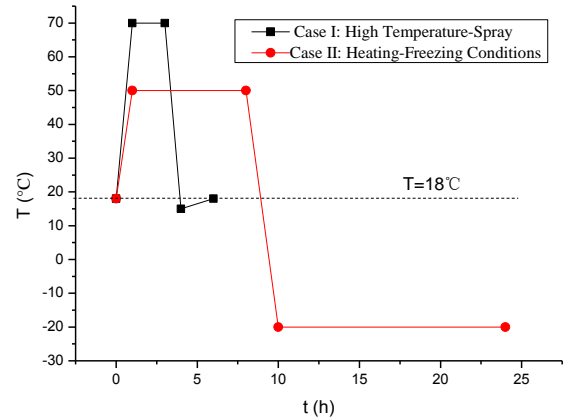


Fig. 3 Surface environmental temperature of wallboard under two working conditions

default setting of ABAQUS is adopted for CFL (Courant-Friedrichs-Lewy) condition of this model: 1) The field equation parameter, R_n^{α} , is 0.005; 2) C_n^{α} is 0.01; 3) \tilde{q}^{α} is equal to 0.01 at the beginning; 4) R_n^{α} is 0.02; and 5) ϵ^{α} is equal to 10^{-5} . For the time increment parameter, I_0 is 4 and I_R is 8.

The grid size of concrete corbel setting is 0.035 m. The grid size of reinforcing mesh, angle steel for connection and FRP connector in RC layer is 0.02 m. The grid size of RC, UHPC and RW is 0.05 m. The time step should be set according to the actual time specified in the weathering test of panel in the test. The initial time step is 60 s, which should be applied automatically. The maximum time step should not exceed the corresponding time of each stage of temperature change.

3.4 Temperature field setting

According to Chinese standard “external wall insulation engineering technical regulations” (JGJ 144-2004) (Vilhena *et al.* 2017) on the external thermal insulation system weatherability: in accelerated weathering test simulating for summer rain and repeated winter and summer temperature difference, it is required that the external wall insulation system should not have empty cover or shedding and should not have decorative layer blister after high temperature water spray and heating refrigeration cycles, and the panel should be able to withstand the outdoor heat, rain and the long-term cycles of cold and hot climate without breaking the ring.

Initial temperature of the wall and the indoor ambient temperature were set at 18 $^{\circ}\text{C}$. At this temperature,

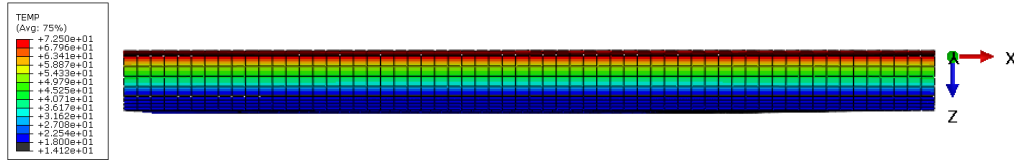


Fig. 4 Temperature distribution of wall panel for 3 hours (case I)

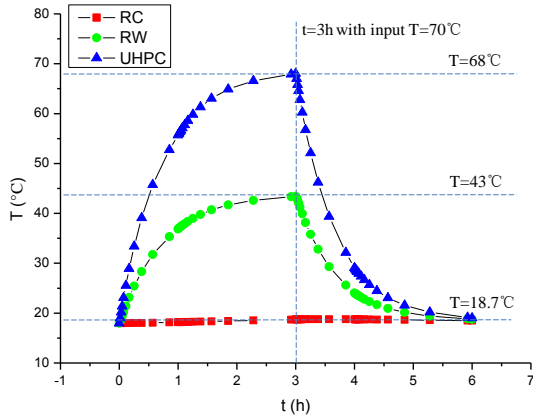


Fig. 5 Temperature time-history curves of RC, RW and UHPC (case I)

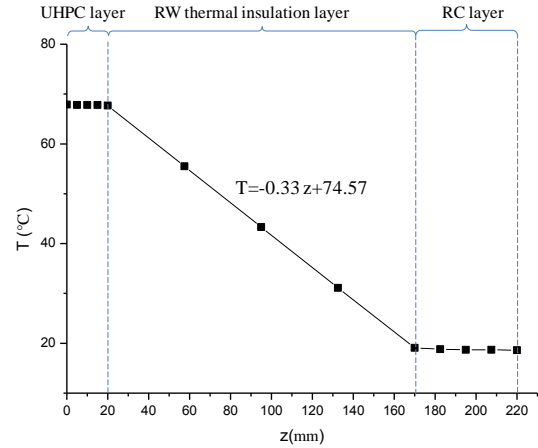


Fig. 6 Temperature distribution (3 hours)

temperature stress of each layer of the wall panel was zero. When the external surface of the wall is subject to the environment, there exists a heat exchange, which is expressed by a heat transfer coefficient and set as the third boundary condition. Ignoring the interlayer thermal resistance, the heat transfer coefficient between the inner surface of the wall and the indoor air is $8.7 \text{ W}\cdot\text{m}^{-2}\cdot\text{°C}^{-1}$, while the heat transfer coefficient between the outer surface of the wall and the outdoor air is $19.0 \text{ W}\cdot\text{m}^{-2}\cdot\text{°C}^{-1}$.

According to the provisions of weathering test for wall panels (Uygunoğlu *et al.* 2016), finite element analysis of temperature stress of the wall panel under high temperature-water spray and heating-freezing conditions was carried out. The ambient temperature of the exterior surface of the wall panel under the conditions of high temperature-water spraying and heating-freezing is shown in Table 2 and Fig. 3.

4. Results and analysis

4.1 Results and analysis of temperature distribution

According to the coordinate axis shown in the model, the points on the two straight lines of general position (1, 0.45, z) and maximum stress position (0.3, 2.85, z) in the wall panel are taken, respectively. The curves of temperature and stress development with time in the middle of UHPC, RW and RC sections are drawn, respectively. The curve of temperature distribution along the wall thickness direction and the curve of stress distribution along the wall thickness direction are drawn with the maximal stress case.

4.1.1 Case I - high temperature-water spray

Temperature distribution of the wall panel under the

action of high temperature and water spray were investigated and are shown in Fig. 4. The temperature curves of UHPC, RW and RC layers are shown in Fig. 5.

From the graph, it can be seen that temperature variation for each layer decreases gradually from outdoor to indoor. The existence of the RW thermal insulation layer significantly weakens heat transfer between the wall layers, and greatly reduces the effect of external temperature changes on the indoor temperature. Temperature of the UHPC outer surface layer varied the most under action of the high temperature and water spray, which varied from 18.0°C to 68.0°C . The surface temperature of RC inner layer had the smallest change. Its temperature varied from 18°C to 18.7°C . The maximum temperature difference between RC inner layer and air indoor was 0.7°C , demonstrating that the wall panel provides good thermal insulation, can maintain the stability of indoor air temperature, and is conducive to the durability of the wall structure layer.

The temperature curve along the wall thickness direction is shown in Fig. 6, and the temperature distribution function along the panel thickness direction can be expressed as

$$T = \begin{cases} 68 & 0 \leq z < 20\text{mm} \\ -0.33z + 74.57 & 20 \leq z < 170\text{mm} \\ 18.7 & 170 \leq z \leq 220\text{mm} \end{cases} \quad (3)$$

From the figure, it can be seen that the most drastic temperature changes in the wall are located at the intersection of UHPC and RW, and RW and RC.

4.1.2 Case II - Heating-freezing

Calculation results of wall panels subject to heating and freezing are shown in Fig. 7.

Temperature curves of the UHPC, RW and RC layers

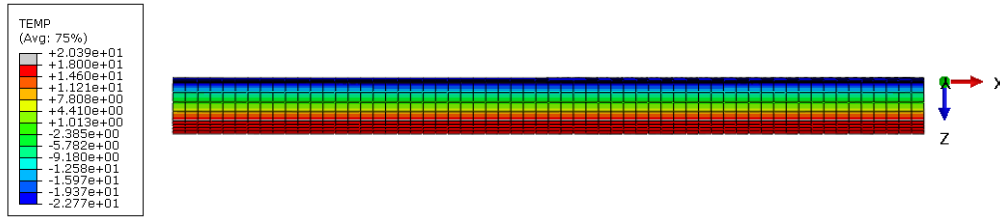


Fig. 7 Temperature distribution of wall panel for 24 hours (case II)

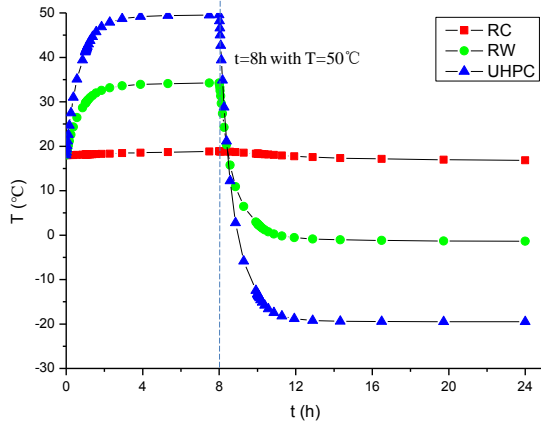


Fig. 8 Temperature time-history curves of RC, RW and UHPC (case II)

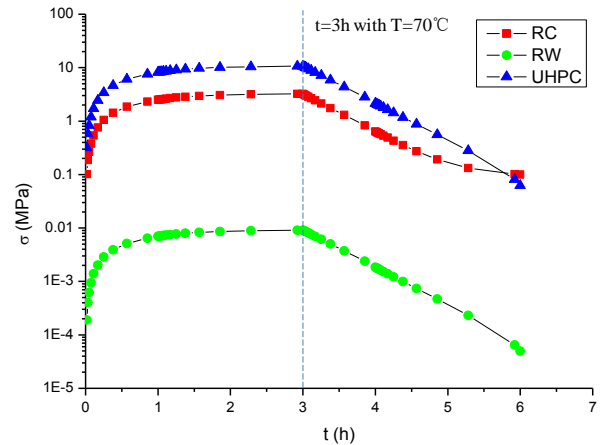


Fig. 10 Stress time-history curve (case I)

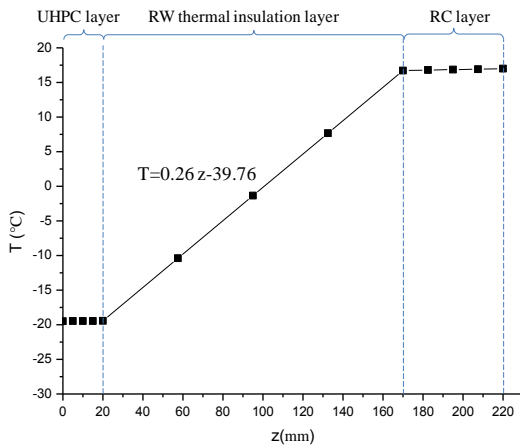


Fig. 9 Temperature distribution (24 hours)

are shown in Fig. 8. It can be seen that the variation of temperature in each structure layer decreases gradually from outdoor to indoor. The existence of RW thermal insulation significantly weakens heat transfer between wall layers, and greatly reduces the effect of external temperature changes on the indoor temperature.

Among the layers, temperature change at the outer surface of UHPC layer is the greatest. During the heating-freezing process, temperature of the UHPC layer ranged from -19.5°C to 49.5°C . The inner surface temperature of RC layer had the smallest change. Its temperature ranged from 16.9°C to 18.8°C . The temperature difference between RC inner layer and air indoor was very small and ranged from -1.1°C to 0.8°C . It shows that the wall panel has good thermal insulation effect and can maintain the stability of indoor air temperature.

Temperature curves along the wall thickness for different temperature stages are shown in Fig. 9. The temperature distribution function along the panel thickness direction can be expressed as

$$T = \begin{cases} -19.5 & 0 \leq z < 20\text{mm} \\ 0.26z - 39.76 & 20 \leq z < 170\text{mm} \\ 18.8 & 170 \leq z \leq 220\text{mm} \end{cases} \quad (4)$$

The results show that the most drastic temperature changes in the wall are located at the intersection of UHPC and RW, RC and RW.

4.2 Results and analysis of stress field

4.2.1 Case I - high temperature-water spray

Stress changes of the wall panels under action of high temperature and water spray were also investigated. The results of which are depicted in Fig. 10.

The stress of the outer UHPC layer was greater than that of the inner RC layer. At the intersection of the outer UHPC layer and the connector, the maximum stress reached 13.9 MPa . For the RC inner layer, maximum stress was also located at its intersection with the connector, where stress value reached 9.3 MPa .

From the von Mises stress distribution curve along the wall thickness (Fig. 11), it can be deduced that the position where stress changes most dramatically is also where temperature changes most dramatically - at the intersection of UHPC and RW and at RW and RC.

From Fig. 12, it can be seen that the stress for most of the UHPC outer layer and RC inner layer is less than their associated cracking strength. But stress in the periphery of the connector is much larger.

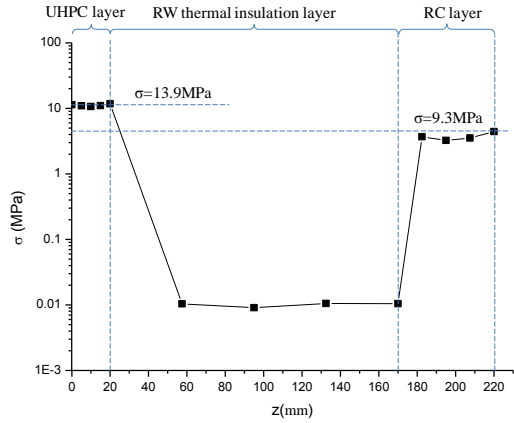


Fig. 11 Stress distribution (12 hours)

Although the temperature difference between the insulation layer and the inner and outer wall layers is relatively large, temperature stress is low due to the RW

layer minor stiffness. The maximum stress of the RW sandwich layer is just 45.8 kPa, which is less than its strength. Thermal stress causes dislocation of the interlayer between the various wall layers.

Stress concentration lies at the joint position, especially at four corner positions for the FRP connection. Here, maximum stress reaches 60.8 MPa, which is far less than the design strength of the connector. Yet, attention to the design of the connector is recommended.

The stress of steel mesh in the inner RC layer was slight, with maximum stress located at the corner of the window hole being 12.7 MPa. Under action of high temperature and water spray, the wall panels did not reach the state of ultimate failure, and for most of the positions not likely to crack.

4.2.2 Case II - Heating-freezing

Under the action of heating and freezing, the temperature stress curves for each layer are shown in Fig. 13. From the figure, large temperature difference between

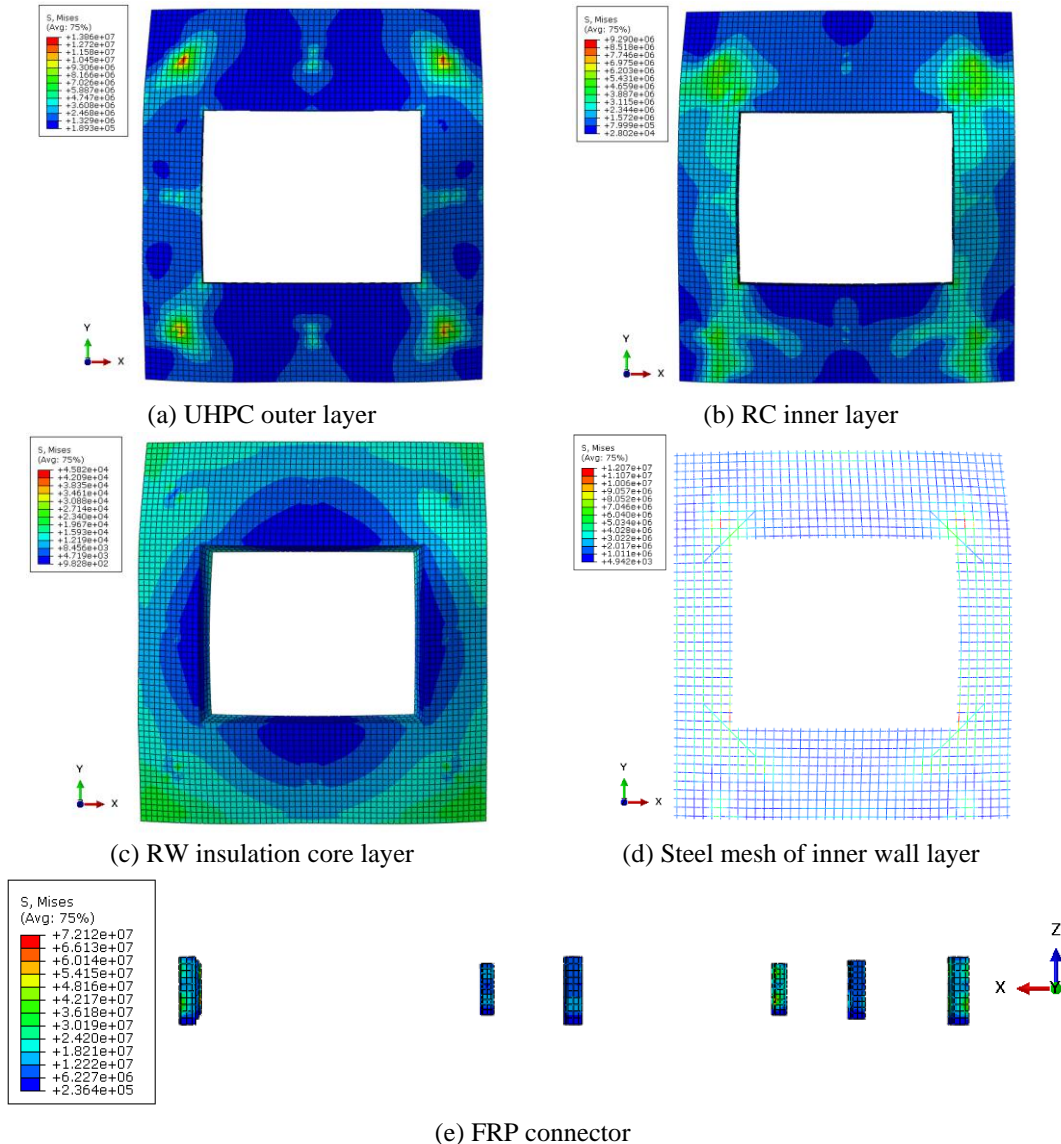


Fig. 12 Stress nephogram under high temperature-water spray (3 hours)

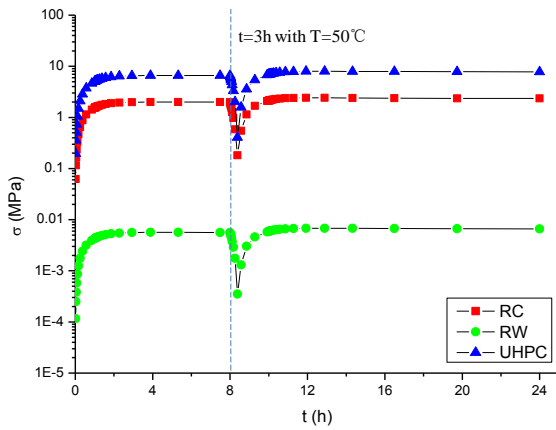


Fig. 13 Stress time-history curve (case II)

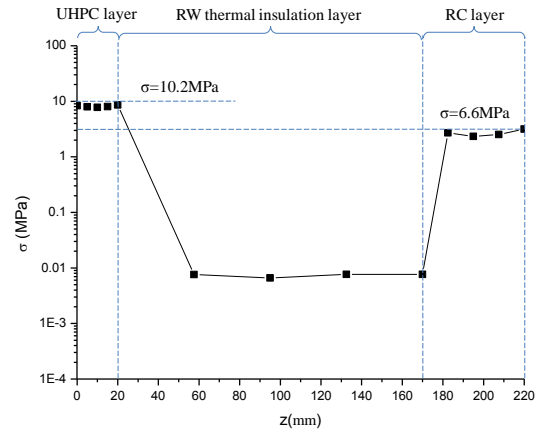


Fig. 14 Stress distribution (24 hours)

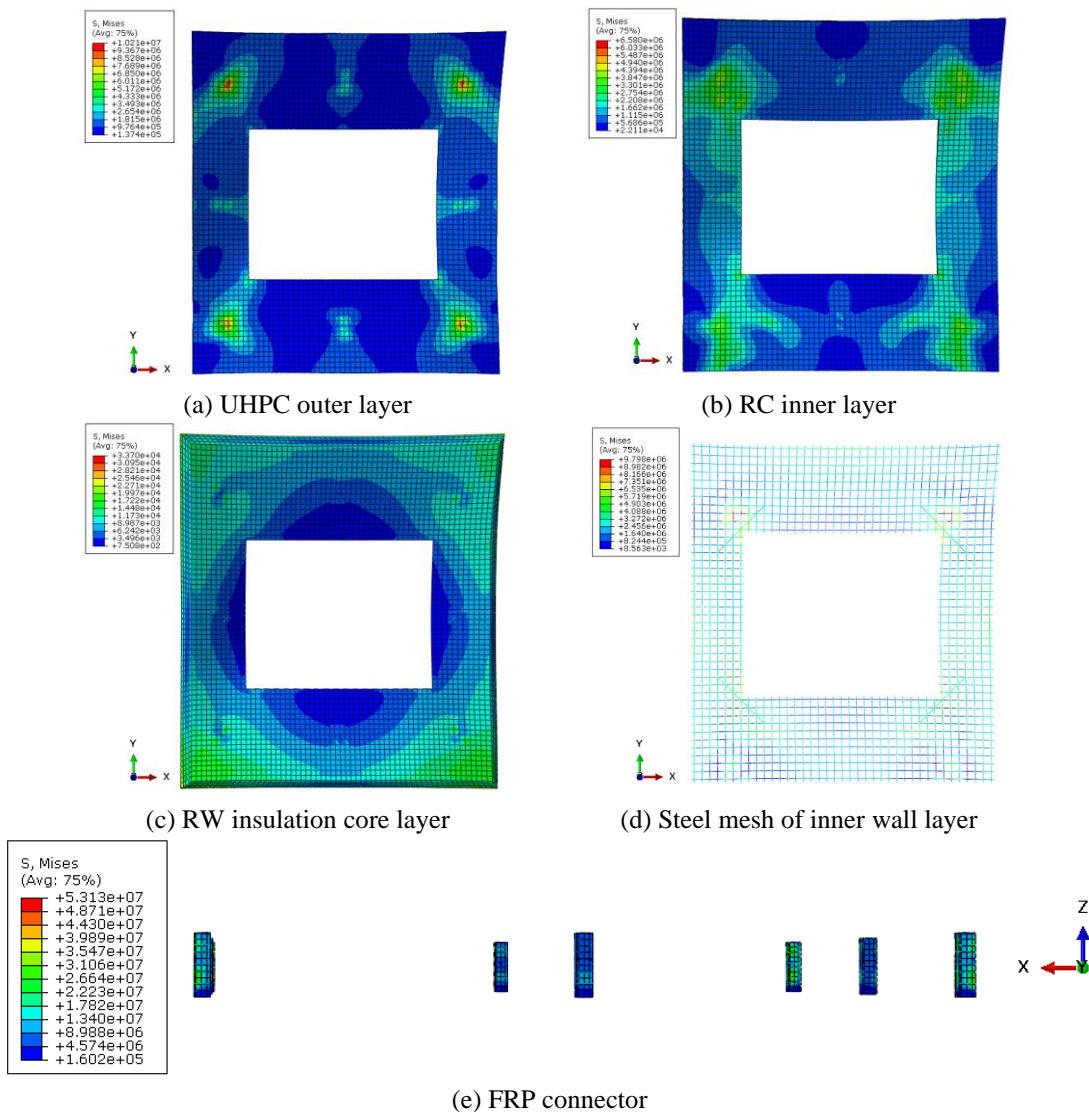


Fig. 15 Stress nephogram under heating-freezing (24 hours)

the connecting parts and the inner and outer wall layers is observed, along with temperature stress. Whether it is heating or freezing, the greater the difference between the wall layer temperature and the initial temperature, the greater the temperature stress.

Although the temperature difference between the insulation layer and the inner and outer wall layers is large, corresponding temperature stress of the inner RC layer is not large due to the small stiffness of the insulation layer itself. During the whole heating-freezing process, the stress

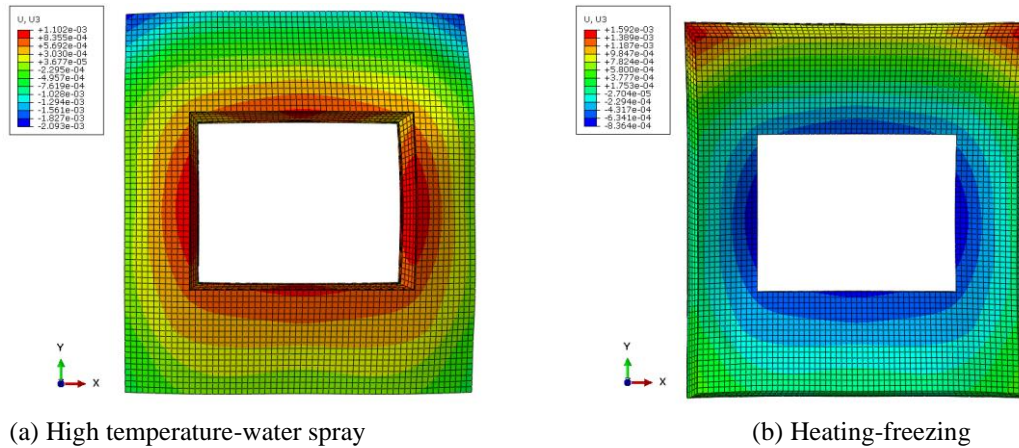


Fig. 16 Displacement nephogram of the wall panel

of the outer UHPC layer was always greater than that of the inner RC layer.

Change of wall stress under heating and freezing conditions was investigated. With increase in temperature, wall stress increased, and when temperature decreased, stress decreased accordingly. In view of the von Mises stress distribution curve along the wall thickness (Fig. 14), the position where stress changed most dramatically similar to that of temperature changes lied at the intersection of UHPC and RW, and at RW and RC.

As shown in Fig. 15, stress at the outer UHPC layer was greater than that of the inner RC layer. Maximum stress lied at the intersection of the outer layer of UHPC and the connector, where stress reached 10.2 MPa. The maximum stress of RC inner layer was also located at the intersection with the connector, and stress there reached 6.6 MPa. Stress in most positions of UHPC outer layer and RC inner layer was less than the cracking strength of UHPC and concrete and thereby not likely to crack. Only stress around the connector was larger.

The maximum stress of the RW sandwich layer was 33.7 kPa, which is less than the strength of RW itself.

The maximum stress of FRP connectors at the four corners reached 53.1 MPa. So extra attention should be paid to the strength of the connectors, although the stress is far less than the design strength of the connectors.

The maximum stress of the steel mesh in the inner layer of RC was located at the corner of the window hole, where it reached 9.8 MPa.

Under the action of heating and freezing, the wall panel will not likely fail, and most of the positions are not likely to crack.

4.3 Displacement analysis

Distribution of displacement field along the thickness direction of the wall after high temperature-water spraying is shown in Fig. 16(a). Maximum displacement shown occurs at the angle of the panel, where it reaches 2.09 mm.

The displacement of the wall panel along the thickness direction of the plate after heating and freezing is shown in Fig. 16(b). There the maximum displacement also occurs at the angle of the panel, where it reaches 1.59 mm.

In both cases, displacement of the wall panel is small, and less than the displacement limit of the wall panel.

4.4 Constructive suggestions

Structural measures should be taken to strengthen the intersection position between connectors and wall layers. To not constrain deformation, a flexible connection should be adopted to connect the wall panels to the main structure, so that ultimate temperature deformation of the external hanging panels and connectors can be absorbed.

Bolt connections with holes to permit displacement adjustment can be arranged at the connection. In addition, a sliding pad can also be added.

5. Conclusions

In this paper, ABAQUS finite element software was used to analyze the temperature and stress field of a composite sandwich wall panel under conditions of high temperature-water spraying and heating-freezing. From that analysis, the following conclusions were drawn:

RW performs well as thermal insulator. It can maintain the stability of indoor air temperature. Under environmental impact, the temperature of the outer layer may greatly, while the temperature of the inner layer remains almost constant, whether in the process of heating or freezing.

The stress of UHPC outer layer is greater than that of RC inner layer. Here, use of a high strength outer layer can improve crack resistance and durability of wall layer.

Maximum stress concentration exists at the intersection of the connector and the outer and inner wall layer. Stress for most positions of UHPC outer layer and RC inner layer was less than the cracking strength of UHPC and concrete and thereby not likely to crack. In addition, RW, connectors and reinforcing steel mesh were found not likely to be damaged.

Given stress concentration was highest at the intersection position between the joints and the wall layers, structure detailing should be strengthened. Flexible joints should be adopted to connect the wall panels and the main structure, so that ultimate temperature deformation of the

external hanging panels and the joints can be absorbed.

Acknowledgments

The work presented in this paper was sponsored by the Key R&D plan of Hebei Province on high tech common key technology tackling and application demonstration special projects (18214903D); HEI Finance (Education) [2012]825; National Natural Science Foundation of China (Grant No. 51678196, 51811540401); National Key R&D Program of China (2018&FC0705400) and Korea Agency for Infrastructure Technology Advancement (KAIA) grant funded by the Ministry of Land, Infrastructure and Transport of Korea (20CTAP-C151831-02).

References

- Bonner, M., Wegrzynski, W., Papis, B.K. and Rein, G. (2020), "Kresnik: a top-down, statistical approach to understand the fire performance of building facades using standard test data", *Build. Environ.*, **169**, 106540. <https://doi.org/10.1016/j.buildenv.2019.106540>.
- GB 50176 (2016), Code for Thermal Design of Civil Building, China Architecture & Building Press, China. (in Chinese)
- JGJ 144 (2004), Technical Specification for External Thermal Insulation on Walls, China Architecture & Building Press, China. (in Chinese)
- JGJ/T 45 (2018), Technical Standard for Application of Precast Concrete Facade Panels, China Architecture & Building Press, China. (in Chinese)
- Lie, T.T. and Kodur, V.K.R. (1996), "Thermal and mechanical properties of steel-fibre-reinforced concrete at elevated temperatures", *Can. J. Civil Eng.*, **23**, 511-517. [https://doi.org/10.1016/0045-7949\(95\)00239-1](https://doi.org/10.1016/0045-7949(95)00239-1).
- Shaikh, F.U.A. and Taweel, M. (2015), "Compressive strength and failure behaviour of fibre reinforced concrete at elevated temperatures", *Adv. Concrete Constr.*, **3**(4), 283-293. <http://dx.doi.org/10.12989/acc.2015.3.4.283>.
- Shin, K.Y., Kim, S.B., Kim, J.H., Chung, M. and Jung, P.S. (2002), "Thermo-physical properties and transient heat transfer of concrete at elevated temperatures", *Nucl. Eng. Des.*, **212**(1), 233-241. [https://doi.org/10.1016/S0029-5493\(01\)00487-3](https://doi.org/10.1016/S0029-5493(01)00487-3).
- Sulakatko, V. and Vogdt, F.U. (2018), "Construction process technical impact factors on degradation of the external thermal insulation composite system", *Sustain.*, **10**(11), 3900. <https://doi.org/10.3390/su10113900>.
- Uygunoğlu, T., Özgüven, S. and Çalış, M. (2016), "Effect of plaster thickness on performance of external thermal insulation cladding systems (ETICS) in buildings", *Constr. Build. Mater.*, **122**(30), 496-504. <https://doi.org/10.1016/j.conbuildmat.2016.06.128>.
- Vilhena, A., Silva, C., Fonseca, P. and Couto, S. (2017), "Exterior walls covering system to improve thermal performance and increase service life of walls in rehabilitation interventions", *Constr. Build. Mater.*, **142**, 354-362. <https://doi.org/10.1016/j.conbuildmat.2017.03.033>.
- Ximenes, S., de Brito, J., Gaspar, P.L. and Silva, A. (2015), "Modeling the degradation and service life of ETICS in external walls", *Mater. Struct.*, **48**(7), 2235-2249.
- Zhang D., Mamesh, Z. Sailauova, D., Shon, C.S., Lee, D. and Kim, J.R. (2019), "Temperature distributions inside concrete sections of renewable energy storage pile foundations," *Applied Sciences*, **9**(22), 1-17. <https://doi.org/10.3390/app9224776>.
- Zhang, B., Cullen, M. and Kilpatrick, T. (2014), "Fracture toughness of high performance concrete subjected to elevated temperatures Part 1 The effects of heating temperatures and testing conditions (hot and cold)", *Adv. Concrete Constr.*, **2**(1), 145-162. <http://dx.doi.org/10.12989/acc.2014.2.2.145>.
- Zhang, B., Cullen, M. and Kilpatrick, T. (2016), "Spalling of heated high performance concrete due to thermal and hygric gradients", *Adv. Concrete Constr.*, **4**(1), 1-14. <http://dx.doi.org/10.12989/acc.2016.4.1.001>.
- Zheng, W., Luo, B. and Wang, Y. (2014), "Microstructure and mechanical properties of RPC containing PP fibres at elevated temperatures", *Mag. Concrete Res.*, **66**(8), 397-408. <https://doi.org/10.1680/macr.13.00232>.

JK